ORIGINAL ARTICLE

Mapping cerebral atrophy and hypometabolism on ^{18}F-FDG PET/CT scans for detecting Alzheimer's disease in the Malaysian population using a Malaysian brain atlas template

Siti Aishah Abdul Aziz, MSc[1,2], Normala Ibrahim, PhD[3], Mohammed Faruque Reza, PhD[4], M. Iqbal Saripan, PhD[2]

[1]School of Health Sciences, Universiti Sains Malaysia, [2]Department of Computer and Communication Systems Engineering, Faculty of Engineering, Universiti Putra Malaysia, [3]Department of Psychiatry, Faculty of Medicine and Health Sciences, Universiti Putra Malaysia, [4]Department of Neurosciences, School of Medical Sciences, Universiti Sains Malaysia

ABSTRACT

Introduction: Studies are lacking in evaluating brain atrophy patterns in the Malaysian population. This study aimed to compare the patterns of cerebral atrophy and impaired glucose metabolism on ^{18}F-FDG PET/CT imaging in various stages of AD in a Klang Valley population by using voxel-based morphometry in SPM12.

Materials and Methods: ^{18}F-FDG PET/CT images of 14 healthy control (HC) subjects (MoCA score > 26 (mean+SD~ 26.93+0.92) with no clinical evidence of cognitive deficits or neurological disease) and 16 AD patients (MoCA ≤22 (mean+SD~18.6+9.28)) were pre-processed in SPM12 while using our developed Malaysian healthy control brain template. The AD patients were assessed for disease severity using ADAS-Cog neuropsychological test. KNE96 template was used for registration-induced deformation in comparison with the ICBM templates. All deformation fields were corrected using the Malaysian healthy control template. The images were then nonlinearly modified by DARTEL to segment grey matter (GM), white matter (WM) and cerebrospinal fluid (CSF) to produce group-specific templates. Age, intracranial volume, MoCA score, and ADAS-Cog score were used as variables in two sample t test between groups. The inference of our brain analysis was based on a corrected threshold of p<0.001 using Z-score threshold of 2.0, with a positive value above it as hypometabolic. The relationship between regional atrophy in GM and WM atrophy were analysed by comparing the means of cortical thinning between normal control and three AD stages in 15 clusters of ROI based on Z-score less than 2.0 as atrophied.

Results: One-way ANOVA indicated that the means were equal for TIV, F(2,11) = 1.310, *p*=0.309, GMV, F(2,11) = 0.923, *p*=0.426, WMV, F(2,11) = 0.158, *p*=0.856 and CSF, F(2,11) = 1.495 *p*=0.266. Pearson correlations of GM, WM and CSF volume between HC and AD groups indicated the presence of brain atrophy in GM (*p*=-0.610, *p*<0.0001), WM (*p*=-0.178, *p*=0.034) and TIV (*p*=-0.374, p=0.042) but showed increased CSF volume (*p*=0.602, *p*<0.0001). Voxels analysis of the 18F-FDG PET template revealed that GM atrophy differs significantly between healthy control and AD (*p*<0.0001). Z-score comparisons in the region of GM & WM were shown to distinguish AD patients from healthy controls at the prefrontal cortex and parahippocampal gyrus. The atrophy rate within each ROI is significantly different between groups (c^2=35.9021, df=3, p<0.0001), Wilcoxon method test showed statistically significant differences were observed between Moderate vs. Mild AD (*p*<0.0001), Moderate AD vs. healthy control (p=0.0005), Mild AD vs. HC (*p*=0.0372) and Severe AD vs. Moderate AD (*p*<0.0001). The highest atrophy rate within each ROI between the median values ranked as follows severe AD vs. HC (*p*<0.0001) > mild AD vs. HC (*p*=0.0091) > severe AD vs. moderate AD (*p*=0.0143).

Conclusion: We recommend a reliable method in measuring the brain atrophy and locating the patterns of hypometabolism using a group-specific template registered to a quantitatively validated KNE96 group-specific template. The studied regions together with neuropsychological test approach is an effective method for the determination of AD severity in a Malaysian population.

KEYWORDS:
Statistical parametric mapping; image preprocessing; DARTEL; neuropsychological test; Malaysian population

INTRODUCTION

Atrophy and hypometabolism in specific grey matter (GM) regions in the brain have been correlated as features of AD. Several studies have been done on GM atrophy showing that early impairment affected the parahippocampal gyrus, precuneus, posterior cingulate, frontal lobe, insula and the cerebellum within a year prior to the diagnosis of AD.[1,2,3] Interestingly, structural neuroimaging had reported that the cerebellum is related to cognition and emotion and has interactions with the cerebral cortex which influences the cognitive deficits in AD patients.[4] The frontal lobes were typically impacted as AD progressed, with symmetrical alterations on both sides.[5] The preserved brain area is usually associated with the occipital and somatosensory cortex including deep cerebral nuclei.[6]

This article was accepted: 01 December 2022
Corresponding Author: Siti Aishah Abdul Aziz
Email: ishah@usm.my

Meguro et al.[7] had replicated the same method by Jobst et al.[8] to configure similar result by Yamaguchi et al.[5] that concluded by measuring the minimum thickness of both sides of the hippocampus denoted as the width of the hippocampus may be used as a benchmark for atrophy pattern in GM with AD. Damage to the medial temporal lobe can cause neurons to lose contact with each other. This may help explain the hypometabolism pattern, especially in the early stages.[9] However, studies are lacking in Asian brain, particularly in the development of Malaysian brain template, which is a pertinent issue that can be caused by potentially differing brain anatomy in terms of size and pattern of atrophy compared to Caucasian brains.[10]

Cortical thickness pattern from Magnetic resonance imaging (MRI) clustering methodology had assisted the determination of atrophy subtypes. This method is combined with ^{18}F-FDG PET/CT analysis to highlight the significant hypometabolism in different regions corresponding to the cortical thinning pattern. Atrophy occurs in the right superior, left inferior, and left middle occipital cortices in the parietal subtype, while in the medial temporal subtype, glucose hypometabolism occurs in the left hippocampus, left inferior orbital frontal, right superior medial frontal, and both caudate regions.[11] However, there is no significant change in the cerebrospinal fluid (CSF) volume in both subtypes of atrophy.[10]

Significant brain atrophy is greater at baseline and 1-year follow-up in Mild cognitive impairment (MCI) converters to Alzheimer's disease (AD), decline in gradient for MCI stable and healthy control, respectively. Continuation of this was the development of AD severity index that is associated with Mini-mental state examination (MMSE), Alzheimer's Disease Assessment Scale–Cognitive (ADAS-Cog), Clinical Dementia Rating Scale Sum of Boxes (CDR-SOB) scale (global and a sum of boxes) and ApoE ε4 status.[12] A cross-sectional study between cognitive function and AD biomarkers had been done by Nathan et al. interpreting their association in the early stage of AD. Unfortunately, they failed to relate any potential moderating factors for instance, the ApoE ε4 status. The Cambridge Neuropsychological Test Automated Battery (CANTAB) method also leave inconclusive results as it was not tested in normal older adults and the volumetric study of the hippocampal was manually done on T1 images without any normalisation to the standard brain size in the population.[9]

Voxel-based morphometry (VBM) permits the evaluation of brain changes or group differences across the whole brain with great regional specificity, without needing an a priori determination of a region of interest (ROI).[13] It involves three basic pre-processing steps 1) tissue classification, 2) spatial normalisation and 3) spatial smoothing, later followed by statistical analysis (Figure 1).

Tissue.classification.segments.the.brain.into.grey.matter (GM), white matter (WM) and CSF. To guarantee voxel-wise comparability, it is necessary to spatially normalise either the individual brain or the native brain segmentation.[14] Aligning magnetic resonance (MR) images of the brain to a reference space is an essential pre-processing step for neuroimaging investigations that requires the use of spatial normalisation. All of the source images must be registered to a common reference image or "template image." Functional imaging investigations rely on the exact spatial placement of brain areas, which is made possible by the one-to-one connection between different brains.[15] The spatial transformation will likely face deformation fields that can be measured by the Jacobian determinant algorithm or DARTEL. The structural brain segments can be corrected by modulated segments (GM, WM and CSF). Lastly, spatial smoothing is applied to degrade the noise by applying a smoothing kernel at full-width-half-maximum (FWHM) between 4-16 mm.

There are currently no specific features in neuroimaging that can address the stages of AD from healthy normal aging. Evidence from previous literatures showed initial GM atrophy occur in the parahippocampal gyrus, precuneus, posterior cingulate, frontal lobe and insula while the National Institute on Aging-Alzheimer's Association workgroups had established guidelines on topographic atrophy of structural MRI in the region of medial, basal and lateral temporal lobes including the medial and lateral parietal cortices.[16] WM atrophy was significant in the corpus collasum, fornix, cingulate WM including the cingulum bundle and parahippocampal clusters.[17] Classical ^{18}F-FDG PET/CT study findings had shown hypometabolism in the lateral temporoparietal cortices, precuneus, posterior cingulate cortices, medial temporal lobes and bilateral hippocampi.[18] We implemented a direct measurement of atrophy and localisation of the patterns of glucose hypometabolism using a group-specific template registered to a quantitatively validated structural MRI KNE96 template to correct for the magnitude of brain deformations in term of the size of Malaysian brains compared with the ICBM 152 template which is used for Caucasians. This Malaysian group-specific template was derived from an optimised VBM method. The Statistical Parametric Mapping, Version 12 software (SPM) analysis with association to neuropsychological test approach was combined with the result from BAAD software (classification of AD using Support Vector Machine) that can predict the progression of AD. Presence of hypometabolism and atrophy on brain pattern analysis is assumed as an effective diagnostic method for AD detection. This study hypothesised that specific atrophy patterns in GM and WM with varying hypometabolism patterns can be used as the reference region for the explicit masking to be applied for an automated analysis. When combined ADAS-Cog scores, it will help in determining the stages of AD.[19]

The BAAD software was developed using VBM logarithmic analysis with the study on the region of interest (ROI) in the common area affected in AD patients. Additional information regarding this software is available from the following website: (http://www.shigamed.ac.jp/hqbioph/BAAD(English)/BAAD.html). This software is reliable due to the fact that it incorporates age as a covariate, which leads to age-corrected z-scores of the hippocampi that are more appropriate for the subject's age.[20]

MATERIALS AND METHODS

Participants

The subjects recruited in total (n=30), were 12 males and 18 females, consisting of 14 Malays, 10 Chinese and 6 Indians over 60 years of age (mean ± SD 9.95+2.73). There were 14

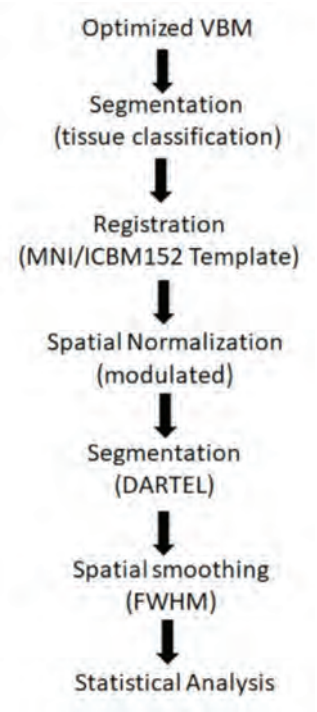

Fig. 1: Flow diagram of the pre-processing steps in an optimised VBM pipeline.

healthy control (HC) subjects and 16 AD subjects in this study. Enrolled HC subjects were volunteers from the same study site who came as escorts to patients or only visited the general clinic. They had no clinical evidence of cognitive deficit or neurological disease, having MoCA scores above 26 (mean±SD 26.93±0.92) and they underwent a standardised protocol of ^{18}F-FDG PET/CT brain scans that showed normal brain anatomy and glucose metabolism.

In brief, the inclusion criteria for AD patients who were recruited as subjects for this study include: (i) the presence of a subjective memory complaint that has been verified using the DSM-5; (ii) a MoCA score of less than 24; and (iii) a clinical diagnosis that sufficiently met the clinical National Institute of Neurological and Communicative Diseases and Stroke/Alzheimer's Disease and Related Disorders Association (NINCDS-ADRDA) criteria for AD. Participants were not allowed to take part if they had a history of serious neurological or psychiatric illnesses, brain malformations, or other conditions that could make it hard for their bodies to break down ^{18}F-FDG. This included taking antidepressants with anticholinergic properties, which could cause problems. Ethical clearance was obtained from the Medical Research Ethics Committee, UPM (JKE-UPM), Human Research Ethics Committee, USM (JEPeM-USM) and Malaysia. The ethical principles conformed with the Helsinki Declaration and were consistent with Malaysian Good Clinical Practice.

The AD patients were screened using MoCA-BM to measure their cognitive deficits. Whereas the severity of the disease was determined using ADAS-Cog. The cut-off score for MoCA-BM was 22 (mean+SD~18.6+9.28) similar to studies conducted in other Asian countries such as Korea and Hong Kong.[15,21] The study also took into consideration of Malaysia's average lower level of educational attainment.[22] Based on the MoCA-BM cut-off scores, there were 3 mild AD subjects, 11 moderate AD subjects and 2 severe AD subjects classified from diagnosis by the clinical psychologists (mean+SD~43.65+12.65). The clinical characteristics of the participants are summarised in Table I.

^{18}F-FDG PET/CT brain analysis

Acquisitions of images were captured using Siemens Truepoint Biograph 64 PET/CT scanner from CDNI, UPM. Statistical analyses were applied using SPM12, whereas image preprocessing and image matrix calculations were done in MATLAB (MathWorks). As the reference brain, KNE96 template was used for registration-induced deformation because of its quantitatively validated Asian templates as opposed to the ICBM152 templates. It was developed by using 96 subjects (M/F=48/48) over 60 years of age (M=69.5±6.2 years old, F = 70.1±7.0 years old).

As there were more than 100% volume variances in the right hemisphere and in the left hemisphere, the use of the ICBM152 template as a reference atlas in Asian populations was unreliable.23 Our calculations also revealed that the differences in the total intracranial volume (TIV) based on Caucasian templates compared with our HC subjects' average brain size was approximately 12.8% and 5.2% larger, using ICBM152 and KNE96 templates, respectively. Therefore, we proceeded to correct all the deformation fields to develop a Malaysian healthy control template based on our 14 participants aged above 60 years old. The deformation field, D is defined by the displacement, d of each voxel point, p and is defined based on:

$$D\,(p) = p + d\,(p) \tag{1}$$

A local relative tissue volume change is measured throughout the brain by the Jacobian operator. It is determined by p as the Jacobian deformation field matrix determinant.[24]

$$Jac_p(D) = \begin{pmatrix} \frac{\partial D_x}{\partial_x} & \frac{\partial D_x}{\partial_y} & \frac{\partial D_x}{\partial_z} \\ \frac{\partial D_y}{\partial_x} & \frac{\partial D_y}{\partial_y} & \frac{\partial D_y}{\partial_z} \\ \frac{\partial D_z}{\partial_x} & \frac{\partial D_z}{\partial_y} & \frac{\partial D_z}{\partial_z} \end{pmatrix} \tag{2}$$

An elementary volume in the source image, denoted by δVsource, is related to its deformed counterpart volume, δVtarget in the target image, using the Jacobian operator.

$$\delta V_{target} = Jac_{\,p}\,(D)\;.\;\delta V_{source} \tag{3}$$

To construct a collection of group-specific templates, the new δV_{target} was nonlinearly modified by the DARTEL technique, and then segmented into GM, WM, and CSF. The images were then warped into the Montreal Neurological Institute (MNI) space using anatomical data from the International Consortium for Brain Mapping (ICBM152) and smoothed using an 8-mm FWHM kernel.

Table I: Clinical characteristics of the participants (n+?)

	Healthy control (N=14)	Alzheimer's disease (N=16)		
		Mild, Mean±SD (n=3)	Moderate, Mean ± SD (n=11)	Severe, Mean±SD (n=2)
Age, Mean±SD (max)	65.9 ± 3.5 (71)	73.7 ± 6.0 (73)	77 ± 6.9 (79)	77.5 ± 0.7 (78)
Education, mean±SD (max)	10.2 ± 2.6 (14)	9 ± 6 (9)	8.7 ± 7.1 (6)	10.5 ± 9.4 (11)
Women subjects (%)	65	67	45	100
MoCA score, mean±SD (max)	26.9 ± 0.9 (28)	20.0 ± 4.0 (24)	10.6 ± 4.8 (20)	5.0 ± 0(5)
ADAS-Cog score, mean±SD (max)	NIL	27.4 ± 2.7 (27)	42.5 ± 6.2 (39)	68.5±2.1 (69)
GMV, mean±SD (max)	1062.4 ± 43.7 (1143.8)	996.9 ± 36.7 (1026.3)	945.2 ± 0 (157.5)	766.1 ± 32.8 (789.3)
WMV, mean±SD (max)	180.4 ± 28.4 (242.6)	179.7 ± 54.4 (240.8)	156.6 ± 132.8 (544.3)	127.5 ± 54.5 (166.1)
CSF, mean±SD (max)	392.6 ± 80.7 (546.5)	468.6 ± 46.2 (521.9)	522.7 ± 36.7 (581.2)	444.1 ± 24.4 (461.33)
TIV, mean±SD (max)	1635.4 ± 83.0 (1804.8)	1645.3 ± 45.3 (1692.7)	1624.2 ± 101.2 (1756.09)	1337.5 ± 46.3 (1370.3)

Table II: Clusters of hypometabolism of subjects in this study (n=?)

Subject	Anatomical region	PFWE-corr	kE	Zscore	Coordinates		
					x	y	z
Healthy control	R superior frontal gyrus medial segment	0.905	516	4.37	9	61	22
	L medial frontal gyrus	0.531	1162	3.89	-35	51	19
	R medial frontal gyrus	0.739	815	3.65	44	44	2
	L cerebral WM	0.999	102	3.47	-36	30	-14
	L caudate	0.997	145	3.26	-18	20	4
	R lateral orbital gyrus	0.999	105	3.25	34	49	-12
Mild AD	L cerebral WM	0.652	169	6.70	-34	2	-14
	R cerebral WM	0.759	151	5.63	8	-54	54
	L fusiform gyrus	0.927	111	5.28	10	8	-12
	R parahippocampal gyrus	0.351	115	4.94	28	-86	42
	R precuneus	0.138	100	3.88	8	-86	34
Moderate AD	L medial temporal gyrus	0.992	140	6.24	-60	-46	-4
	R cerebral WM	0.976	228	5.83	44	-50	20
	RL posterior cingulate gyrus	0.976	228	3.40	-4	-42	26
	L lateral ventricle	0.992	116	3.36	-26	-50	20
	R medial temporal gyrus	0.998	119	3.19	52	-8	-18
	R lingual gyrus	0.998	103	3.16	12	-56	6
Severe AD	R/L cerebrum	0.999	435	7.31	-14	8	10
	R Superior temporal gyrus	0.992	316	6.75	-46	16	-14
	R Inferior temporal gyrus	0.872	212	5.23	6	12	-18
	L temporal lobe	0.992	286	5.73	-54	12	-6
	L cerebellum	0.766	197	5.44	12	18	-16
	R cerebellum	0.513	173	5.16	-28	-42	-24
	Middle occipital lobe	0.511	165	4.47	4	60	-18
	R fusiform gyrus	0.508	149	4.38	36	-49	-8

Comparisons of cerebral atrophy based on hypometabolic regions
Pre-processed images were further analysed using BAAD software for ROI-wise analysis using preset ROIs for automated anatomical labelling (AAL). Volume at the local level was modified, taking into account both TIV and chronological age. Since it was already known from experience that TIV cancelled out sex differences, we decided not to include sex as a covariate in our analysis. With age and TIV as confounders, BAAD used the 60+ age group in the IXI database as a reference to figure out z-scores.[20] In order to estimate the atrophy level for each AD group, z-score were calculated based on gray matter volume (GMV) and white matter volume (WMV) adjusted to the mean volume of healthy controls.

The z-score maps were displayed as an overlay on tomographic sections and surface renderings of the standardised 3D MRI brain in the software. Next, the volume loss was compared between mild AD, moderate AD and severe AD. Two-sample T-test analysis showed that covariates for factorial design were TIV and MoCA scores. ADAS-Cog scores were added for the AD group analysis. Significance for voxel was accepted at a corrected threshold of $p<0.001$ for GM, WM, and CSF comparisons versus healthy controls and an uncorrected threshold of $p<0.001$ for AD group comparisons. The Z-score map of 118 ROIs for GM and 23 ROIs of WM were compared between healthy control and the AD groups.

RESULTS

Voxel Analysis Using SPM
Based on Table II, the comparison with healthy control and AD patients showed a significant hypometabolic region at

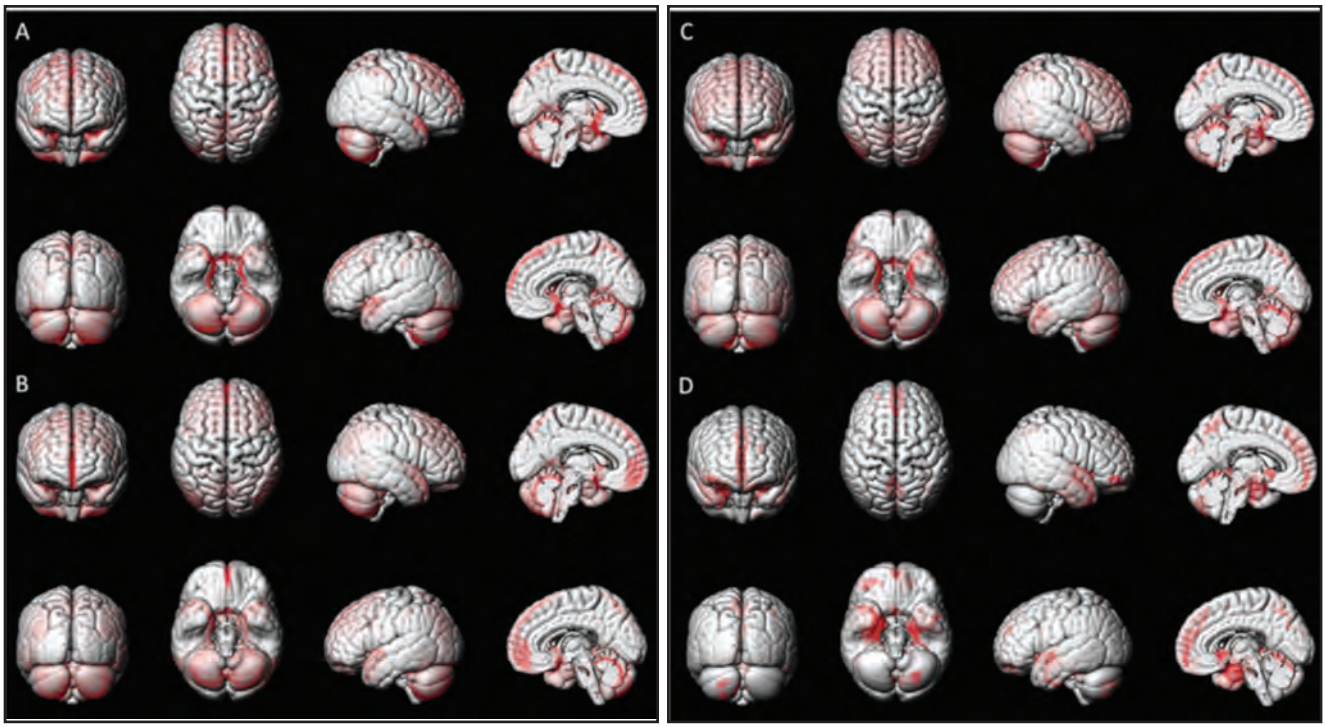

Fig. 2: Grey matter atrophy and white matter hyperintensities between all groups adjusted by total intracranial volume (TIV) and age; (A) Healthy control, (B) Mild AD, (C) Moderate AD, and (D) Severe AD. (Clusters of ROI are specified at 50 voxels with Z-score for voxel numbers (Z<=2.0) of ROI.)

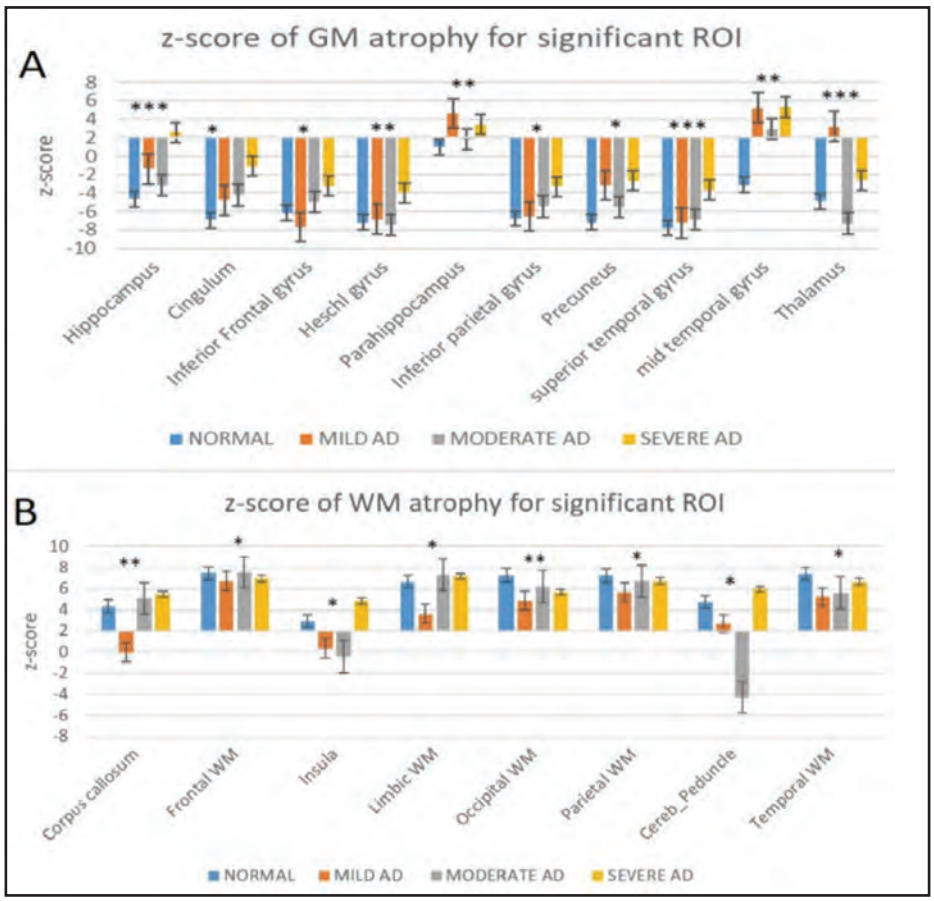

Fig. 3: Z-score of significant ROI showing atrophy in healthy control, mild AD, moderate AD and severe AD. Z-score of significant ROI showing atrophy in the GM (A). Z-score of significant ROI showing atrophy in the WM (B).
*Z score were compared using single-factor ANOVA. **When significance was ($p<0.05$), post hoc analysis was performed using Dunn All Paris for Joint Ranks (*$p<0.05$; **$p<0.005$;***$p<0.0001$).

the frontal, medio-temporal, hippocampal and parahippocampal gyrus. Comparisons within AD groups revealed a more widespread pattern of a hypometabolic region or distinct atrophy of GM and WM hyperintensity especially at the frontal, bilateral temporal, medio-temporal and parietal lobe.

Results based on one-way ANOVA indicated that the means were equal for TIV, $F(2,11) = 1.310$, $p=0.309$, GMV, $F(2,11) = 0.923$, $p=0.426$, WMV, $F(2,11) = 0.158$, $p=0.856$ and CSF, $F(2,11) = 1.495$ $p=0.266$. Therefore, we combined all of our healthy normal participants for the derivation of the Malaysian template. Comparisons between templates revealed different patterns were visualised between ICBM152, KNE96 and ^{18}F-FDG PET Malaysian template. Pearson correlations of GM, WM and CSF volume between healthy control and AD groups indicated that brain atrophy in GM ($p=-0.610$, $p<0.0001$), WM ($p=-0.178$, $p=0.034$) and TIV ($\rho=-0.374$, $p=0.042$) but the increased volume of CSF ($\rho=0.602$, $p<0.0001$).

One-way ANOVA between-group analysis was done selecting the TIV, MoCA-BM scores and ADAS-Cog scores as the covariates. Our results displayed in Table II were similar to previous works in locating the hypometabolic region of HC and AD brains.[2,4,25,26,27] The atrophy and WM hyperintensities between these groups were compared from the result of BAAD software, as shown in Figure 2.

Statistical Analyses

The relationship between regional atrophy in grey matter and white matter atrophy was analysed by comparing the means between normal control and three AD stages using all the criteria stated by Syaifullah et al.[20] The statistical analysis was run in SPSS version 26.0. As the sample size is small, the normality test using the Shapiro-Wilk test showed a significant difference between grey matter and white matter volume with the atrophy rate and atrophy weight in all the ROIs in AAL. To study the regional GM and WM atrophy effect on different groups of AD, analysis of means for Variances-Levene (ADM) were done on GM and WM regional volumes to select the region that falls outside the lower decision limit from the analysis of means charts. The GM clusters are the cingulum, hippocampus, inferior frontal gyrus, Heschl gyrus, parahippocampus, inferior parietal gyrus, medial temporal gyrus and thalamus. The WM clusters are corpus callosum, frontal, insula, limbic, occipital, parietal, peduncle and temporal region. Total GM and WM cluster to be considered are 15 clusters.

The correlations between variables were made using Spearman's ρ and Kendall's tau as the data showed a non-normal distribution. There was a strong, positive correlation between atrophy weight of ROI in a whole-brain with the atrophy rate within each ROI, ($p=0.8025$, $p<0.0001$), ($\tau_b=0.6242$, $p<0.0001$) but less significant correlations between the reduced volumes of each ROI with the atrophy weight of ROI in a whole brain with the atrophy rate within each ROI. Consequently, there is a significant correlation between the z-score of each ROI and the atrophy rate within each ROI ($p=0.5803$, $p<0.0001$), ($\tau b=0.4124$, $p<0.0001$), whereas a negative strong correlation between the z-score of each ROI and the regional volume ($p=-0.7011$, $p<0.0001$), ($\tau_b=-0.5161$, $p<0.0001$). Kruskal–Wallis H tests were conducted to examine the differences in the atrophy indicators among the three groups with healthy controls. Significant difference was found by chi-square approximation; consequently, the Wilcoxon method test was employed to generate a nonparametric pairwise comparison, and Dunn All-Patients for Joint Ranks was utilised to assess if the post hoc tests were significant.

The atrophy rate within each ROI is significantly different between groups from the chi-square approximation (2=35.9021, df=3, $p<0.0001$), Wilcoxon method test showed statistically significant differences were observed between Moderate vs. Mild AD ($p<0.0001$), Moderate AD vs. healthy control ($p=0.0005$), Mild AD vs. healthy control ($p=0.0372$) and Severe AD vs. Moderate AD ($p<0.0001$). The highest atrophy rate within each ROI between the median values ranked as follows severe AD vs. healthy control ($p<0.0001$) > mild AD vs. healthy control ($p=0.0091$) > severe AD vs. moderate AD is ($p=0.0143$). This result indicates that atrophy is the major indicator in the diagnosis of AD in grey matter and white matter shown in Figures 3A and 3B.

DISCUSSION

Our objective was to characterise the atrophy patterns from statistical parametric testing and incorporate the information from MoCA-BM and ADAS-Cog in diagnosing the severity of AD among Malaysians. The neuropsychological test result of the ADAS-Cog results showed that the risk of AD is not covariate with age and formal education. Based on the three stages of severity of AD, our study showed that MoCA and ADAS-Cog was inversely correlated with increasing severity of AD.

Our study emphasised on categorising AD patients based on ADAS-Cog and the location of peak intensity signals on ^{18}F-FDG PET/CT from more than 100 voxels per cluster that had shown the correlation between these signals with the important cognitive functional parts in the brain.

We used the newly validated KNE96 template instead of the ICBM152 template to correct for all the global brain shapes and sizes of the Malaysian population as computational neuroimaging studies that interpret the anatomical features using an unsuitable template may lead to false study results.[28] The inference of our brain analysis was based on a corrected threshold of $p<0.05$ at Z-score threshold of 2.0 with a positive value above it as hypometabolic in agreement with a study done by Oshikubo et al. on his voxel-based specific regional analysis system for Alzheimer's disease (VSRAD) combined with the Japanese version of the Neurobehavioral Cognitive Status Examination (COGNISTAT).[27] The threshold level was set higher than previous findings due to our age-specific ROIs with modulated VBM.[28] Healthy control showed a distinct hypometabolism pattern at the frontal part of the brain whilst the early stage of AD indicated that hypometabolic areas were concentrated at temporal, hippocampal and parahippocampal gyrus. It was also observed that healthy control and AD diagnostic group have similarities in the hypometabolic area detected in clusters of more than 100 voxels with reduced activity in multiple sites of the brain when neuropsychological test results were taken into account (Figure 2).

To the best of our knowledge, this 18F-FDG PET/CT template was the first that was developed in a multi-ethnicity population pool. The small sample size collected degrades the co-registered brain images for each sample that does not correspond to the true shape of GM and WM as compared to the ICBM152 and KNE96 templates. Thus, hypometabolic regions appeared diffused to the deep brain from the 'real grey matter' region. Nonetheless, the incomplete registration to the reference template using the standard VBM was responsible for the differences in deep brain GM findings.[20] A study done by Bhalerao et al. on MRI brain of 15 Indian subjects to evaluate the registration accuracy differences between MNI, Chinese-56 and Indian templates had found out that the MNI-152 template was larger than that of both Chinese and Indian templates (p<0.001), whereas there were no significant differences between the Chinese template and MNI template (p=0.87). Global brain differences have demonstrated that the non-Caucasian subject spatial normalisation data were unsuitable using the MNI template.[10] However in this study, using the KNE96 template as the reference image, our Malay, Indian and Chinese healthy control participants' brain volume did not show a statistically significant difference.

Voxels analysis of the ^{18}F-FDG PET template revealed that GM atrophy with z-score of each ROI threshold at z<=2.0 differs significantly between healthy control and AD at the hippocampus, superior temporal gyrus and thalamus (p<0.0001). Z-score comparisons in the region of GM have been shown to distinguish mild AD patients from healthy control at the prefrontal cortex, parahippocampal gyrus, Heschl gyrus and medial temporal gyrus.[27,29] These region were the best discriminator in the preclinical stage of AD which supported a recent report pertaining entorhinal cortex and parahippocampus as the earliest region affected using texture analysis.[21] The medial temporal lobe atrophy associated with cognitive outcome is a consistent finding with earlier observations of patients with or without mild cognitive impairment.[30] The medial temporal gyrus comprising of hippocampus, entorhinal cortex, perirhinal cortex and parahippocampal cortex are the subregions critical for cognitive functions because they are the primary target of neurofibrillary tangles that are characteristics for the diagnosis of AD.[31]

Significant WM atrophy was observed in corpus callosum and insula in mild AD, while cerebral peduncle and insula were the significant WM atrophy region in worsened AD condition. These findings corroborate with results from a recent study that concludes amyloid beta plaque accumulation was associated with WM alterations mainly in corpus callosum, percuneus and insula.[32] Research into the WM changes in AD may clarify the pathophysiological mechanisms underlying neuropsychological and anatomical asymmetry. The effect of diffusivity of WM spreads bilaterally in the parahippocampal gyrus and temporal lobes.[21] Within the prefrontal cortex, the WM was particularly susceptible to age-related and cognitive decline in AD patients compared to the GM. It was also known that WM loss was selective as the volumetric measurements were less in older age AD, > 80 years compared to younger age AD, <70 years.[33] Another study also found that early indication of AD also includes WM atrophy was focused on cingulum bundle, parahippocampal clusters corresponding to the prefrontal and temporal WM clusters similar with our result in Figure 3(b).[26,34]

Acknowledgement of the atrophy pattern helps determine the advanced state of AD and can serve as biomarkers to forecast the future development of Alzheimer's disease-induced subjects. It should be noted that the clinical presentation and the actual level of glucose hypometabolism in the AD brain are still highly varied.

LIMITATIONS

The limitations of this study arise from firstly, the limited sample size. This single-centred study for the major population of Klang Valley with a convenience sampling method introduced sampling bias for representation of the Malaysian population. Therefore, multiple sites' involvement with larger sample sizes is suggested to understand the pattern of ^{18}F-FDG metabolism, for accurate co-registration of a standard brain for various ethnicity in Malaysia. Secondly, the spatial normalisation of our template does not match the reference MNI PET template which might introduce failure of exact morphological characteristics on an individual brain.

Our ^{18}F-FDG PET template suffers from non-rigid brain registration due to its low resolution and "spatial normalization" for each individual that failed to match the reference MNI PET template. The appearance of GM and WM volumes does not correspond to the true shape as registered to MRI T1-weighted image in ICBM152 and KNE96 template. This was due to the template used for SPM normalisation being based on oxygen-15-labelled water PET (15O-H20 PET) images that neither corresponds to the metabolic feature of ^{18}F-FDG brain scans nor the specific morphological characteristics of individual AD brain.[26]

For future studies, the development of brain templates of 18F-FDG PET/CT based on specific patient ethinicity for the development of a common stereotaxic space using DARTEL will help to improve automated image analysis, tissue classification and region of interest analysis.

CONCLUSION

Our study confirms the pattern of brain atrophy and hypometabolic regions of Alzheimer's disease subjects with reference to the ^{18}F-FDG PET/CT in a Malaysian brain template. It has an important diagnostic value and is a promising method with combination of MoCA and ADAS-Cog score as an effective method not only for the diagnosis but also in the assessment of the severity of disease in patients with AD in a multi-ethnicity Malaysian population. Our study has proven that the widespread of GM hypometabolism and distinct atrophy in the frontal, bilateral temporal, medio-temporal and parietal lobe are significant with WM atrophy of the insula region in all AD stages. This deciphered what has been the signature of AD severity marker compared with the healthy control. The correlation of z-score of each ROI with atrophy rate and brain regional volume is the major indicator in determining the AD severity.

ACKNOWLEDGEMENTS

This study was funded by Bridging Grant: Universiti Sains Malaysia (304.PPSK.6316218) and Geran Penyelidikan Individu Berprestasi Tinggi-Putra: Universiti Putra Malaysia (940990).

REFERENCES

1. Meguro K, LeMestric C, Landeau B, Desgranges B, Eustache F, Baron JC. Relations between hypometabolism in the posterior association neocortex and hippocampal atrophy in Alzheimer's disease: a PET/MRI correlative study.J Neurol Neurosurg Psychiatry 2001; 71(3): 315-21.
2. Spulber G, Niskanen E, Macdonald S, Kivipelto M, Padilla DF, Julkunen V, et al. Evolution of global and local grey matter atrophy on serial MRI scans during the progression from MCI to AD.Curr Alzheimer Res 2012; 9(4): 516-24.
3. Takahashi R, Ishii K, Miyamoto N, Yoshikawa T, Shimada K, Ohkawa S, et al. Measurement of gray and white matter atrophy in dementia with lewy bodies using diffeomorphic anatomic registration through exponentiated lie algebra: A comparison with conventional voxel-based morphometry.Am J Neuroradiol 2010; 31(10): 1873-8.
4. Jacobs HIL, Hopkins DA, Mayrhofer HC, Bruner E, van Leeuwen FW, Raaijmakers W, et al. The cerebellum in Alzheimer's disease: evaluating its role in cognitive decline.Brain 2018; 141(1): 37-47.
5. Yamaguchi S, Meguro K, Itoh M, Hayasaka C, Shimada M, Yamazaki H, et al. Decreased cortical glucose metabolism correlates with hippocampal atrophy in Alzheimer's disease as shown by MRI and PET.J Neurol Neurosurg Psychiatry 1997; 62(6): 596-600.
6. Silverman DHS. Brain 18 F-FDG PET in the Diagnosis of Neurodegenerative Dementias: Comparison with Perfusion SPECT and with Clinical Evaluations Lacking Nuclear Imaging*.J Nucl Med 2004; 45(4): 594-607.
7. Meguro K, Lemestric C, Landeau B, Desgranges B, Eustache F, Baron JC. Relations between hypometabolism in the posterior association neocortex and hippocampal atrophy in Alzheimer's disease: a PET/MRI correlative study. J Neurol Neurosurg Psychiatry 2001; 71: 315-21.
8. Jobst KA, Smith AD, Barker CS, Wear A, King EM, Smith A, et al. Association of atrophy of the medial temporal lobe with reduced blood flow in the posterior parietotemporal cortex in patients with a clinical and pathological diagnosis of Alzheimer's disease.J Neurol Neurosurg Psychiatry 1992; 55(3): 190-4.
9. Nathan PJ, Lim YY, Abbott R, Galluzzi S, Marizzoni M, Babiloni C, et al. Association between CSF biomarkers, hippocampal volume and cognitive function in patients with amnestic mild cognitive impairment (MCI). Neurobiol Aging 2017; 53: 1-10.
10. Bhalerao GV, Parlikar R, Agrawal R, Shivakumar V, Kalmady S V, Rao NP, et al. Construction of population-specific Indian MRI brain template: Morphometric comparison with Chinese and Caucasian templates.Asian J Psychiatr 2018; 35: 93-100.
11. Hwang J, Kim CM, Jeon S, Lee JM, Hong YJ, Roh JH, et al. Prediction of Alzheimer's disease pathophysiology based on cortical thickness patterns.Alzheimer's Dement Diagnosis, Assess Dis Monit 2015; 2: 58-67.
12. Hwang J, Kim CM, Jeon S, Lee JM, Hong YJ, Roh JH, et al. Prediction of Alzheimer's disease pathophysiology based on cortical thickness patterns.Alzheimer's Dement Diagnosis, Assess Dis Monit 2016; 2: 58-67.
13. Ashburner J, Friston KJ. Voxel-based morphometry - The methods.Neuroimage 2000; 11(6 I): 805-21.
14. Lee JY, Lee DW, Cho SJ, Na DL, Jeon HJ, Kim SK, et al. Brief screening for mild cognitive impairment in elderly outpatient clinic: validation of the Korean version of the Montreal Cognitive Assessment.J Geriatr Psychiatry Neurol 2008; 21(2): 104-10.
15. Chu LW, Ng KHY, Law ACK, Lee AM, Kwan F. Validity of the Cantonese Chinese Montreal Cognitive Assessment in Southern Chinese.Geriatr Gerontol Int 2015; 15(1): 96-103.
16. Jack CRJ, Albert MS, Knopman DS, McKhann GM, Sperling RA, Carrillo MC, et al. Introduction to the recommendations from the National Institute on Aging-Alzheimer's Association workgroups on diagnostic guidelines for Alzheimer's disease.Alzheimers Dement 2011; 7(3): 257-62.
17. Villain N, Desgranges B, Viader F, de la Sayette V, Mézenge F, Landeau B, et al. Relationships between hippocampal atrophy, white matter disruption, and gray matter hypometabolism in Alzheimer's disease. J Neurosci 2008; 28(24): 6174-81.
18. Nasrallah IM, Wolk DA. Multimodality imaging of Alzheimer disease and other neurodegenerative dementias. J Nucl Med 2014; 55(12): 2003-11.
19. Zainal NH, Silva E, Lim LL, Kandiah N. Psychometric Properties of Alzheimer's Disease Assessment Scale-Cognitive Subscale for Mild Cognitive Impairment and Mild Alzheimer's Disease Patients in an Asian Context. Ann Acad Med Singapore 2016; 45: 273-83.
20. Syaifullah AH, Shiino A, Kitahara H, Ito R, Ishida M, Tanigaki K. Machine Learning for Diagnosis of AD and Prediction of MCI Progression From Brain MRI Using Brain Anatomical Analysis Using Diffeomorphic Deformation. Front Neurol 2021; 11: 1894.
21. Freitas S, Simões MR, Alves L, Santana I. Montreal Cognitive Assessment: validation study for mild cognitive impairment and Alzheimer disease. Alzheimer Dis Assoc Disord 2013; 27.
22. Aziz SAA, Saripan MI, Ibrahim N, Saad FFA, Suppiah S, Ismail SIF, et al. Combining ADAS-Cog Assessment with Hypometabolic Region of 18F-FDG PET/CT Brain Imaging for Alzheimer's Disease Detection. In: 2020 IEEE-EMBS Conference on Biomedical Engineering and Sciences (IECBES) 2021: 166-71.
23. Lee H, Yoo B Il, Han JW, Lee JJ, Oh SYW, Lee EY, et al. Construction and validation of brain MRI templates from a Korean normal elderly population. Psychiatry Investig 2016; 13(1): 135-45.
24. Shen S, Sterr A. Is DARTEL-based voxel-based morphometry affected by width of smoothing kernel and group size? A study using simulated atrophy. J Magn Reson Imaging 2013; 37(6): 1468-75.
25. Aziz SAA, Ling LJ, Saad FFA, Nordin AJ, Ibrahim N, Nuruddin A, et al. Voxel-wise analysis of 18F-fluorodeoxyglucose metabolism in correlation with variations in the presentation of Alzheimer's disease: a clinician's guide. Med J Indones 2019; 28(3 SE-Brief Communication).
26. Della Rosa PA, Cerami C, Gallivanone F, Prestia A, Caroli A, Castiglioni I, et al. A Standardized [^{18}F]-FDG-PET Template for Spatial Normalization in Statistical Parametric Mapping of Dementia.Neuroinformatics 2014; 12(4): 575–93.
27. Oshikubo G, Akahane A, Unno A, Watanabe Y, Ikebuchi E, Tochigi M, et al. Utility of VSRAD for diagnosing Alzheimer's disease in patients screened for dementia.J Int Med Res. 2020;
28. Matsunari I, Samuraki M, Chen WP, Yanase D, Takeda N, Ono K, et al. Comparison of 18F-FDG PET and Optimized Voxel-Based Morphometry for Detection of Alzheimer's Disease: Aging Effect on Diagnostic Performance. J Nucl Med 2007; 48(12): 1961-70.
29. Echávarri C, Aalten P, Uylings HBM, Jacobs HIL, Visser PJ, Gronenschild EHBM, et al. Atrophy in the parahippocampal gyrus as an early biomarker of Alzheimer's disease. Brain Struct Funct 2011; 215(3-4): 265-71.
30. Clerx L, van Rossum IA, Burns L, Knol DL, Scheltens P, Verhey F, et al. Measurements of medial temporal lobe atrophy for prediction of Alzheimer's disease in subjects with mild cognitive impairment. Neurobiol Aging 2013; 34(8): 2003-13.
31. Chauveau L, Kuhn E, Palix C, Felisatti F, Ourry V, de La Sayette V, et al. Medial Temporal Lobe Subregional Atrophy in Aging and Alzheimer's Disease: A Longitudinal Study. Front Aging Neurosci 2021; 13.
32. Phillips O, Joshi SH, Piras F, Orfei MD, Iorio M, Narr KL, et al. The Superficial White Matter in Alzheimer's Disease. Hum Brain Mapp 2016; 37(4): 1321-34.
33. Mahanand BS, Kumar AM. Analysis of Alzheimer's Disease Progression in Structural Magnetic Resonance Images. WSEAS Trans Comput 2009; 8(4, April): 579-88.
34. Serra L, Cercignani M, Mastropasqua C, Torso M, Spanò B, Makovac E, et al. Longitudinal Changes in Functional Brain Connectivity Predicts Conversion to Alzheimer's Disease. J Alzheimers Dis 2016; 51(2): 377-89.